

An inter-laboratory comparison of EPMA analysis of alloy steel at low voltage

This article has been downloaded from IOPscience. Please scroll down to see the full text article.

2012 IOP Conf. Ser.: Mater. Sci. Eng. 32 012014

(<http://iopscience.iop.org/1757-899X/32/1/012014>)

View [the table of contents for this issue](#), or go to the [journal homepage](#) for more

Download details:

IP Address: 161.116.19.2

The article was downloaded on 16/03/2012 at 08:19

Please note that [terms and conditions apply](#).

An inter-laboratory comparison of EPMA analysis of alloy steel at low voltage

X Llovet^{1,8}, E Heikinheimo², A Núñez Galindo³, C Merlet⁴, J F Almagro Bello³, S Richter⁵, J Fournelle⁶ and C J G van Hoek⁷

¹ University of Barcelona, Centres Científics i Tecnològics (CCiT), C/ Lluís Solé i Sabarís 1-3, ES-08028 Barcelona, Spain

² Aalto University, Department of Materials Science and Engineering, P.O. Box 16200, FI-00076 Aalto, Espoo, Finland

³ Acerinox S.A., Departamento I+D+i, Pol. Industrial Palmones s/n, ES-11319 Los Barrios, Spain

⁴ Université de Montpellier II, CNRS, Laboratoire Géosciences Montpellier, Place Eugène Bataillon, FR-34095 Montpellier Cedex 5, France

⁵ RWTH Aachen University, GFE - Central Facility for Electron Microscopy, Ahornstrasse 55, DE-52074 Aachen, Germany

⁶ University of Wisconsin, Department of Geoscience, 1215 West Dayton Street, US-53706 Madison, Wisconsin, U.S.A.

⁷ Tata Steel Europe, RD&T, Ceramic Research Centre, P.O. Box 10.000, NL-1970 CA IJmuiden, The Netherlands

E-mail: xavier@ccit.ub.edu

Abstract. We present the results of an inter-laboratory comparison of EPMA analysis at low voltage (5 - 6 kV) of three monophasic alloy steel samples. The aim of the work was to obtain an estimate of the present situation of low-voltage analysis of steel and identify needs for improvement. EPMA analyses of the samples were conducted by seven participant groups using electron microprobes and scanning electron microscopes of different kind, equipped with wavelength- and/or energy-dispersive X-ray spectrometers, and employing their own methodology of analysis. The results using WDS showed essentially an underestimation of the Cr contents, with relative deviations from the reference values ranging from -0.7 % to -17 %, and an overestimation of Fe and Ni, with relative deviations from the reference composition ranging from -4 % to +30 %, and from +14 % to +42 %, respectively. The relative deviations obtained by using EDS showed larger scatter, ranging from -16 % to +54 % for Cr, -0.4 % to +66 % for Fe and from +13 % to +90 % for Ni. Reasons for the differences observed and the scatter of results are discussed.

1. Introduction

Modern electron beam instruments coupled with field-emission electron guns (FEG) have opened new opportunities to perform electron probe microanalysis (EPMA) at low voltages (< 10 kV). At such energies, the penetration range of incident electrons drops from the conventional micrometre scale

⁸ To whom any correspondence should be addressed.

down to the sub-micrometre scale, and leads to a significant improvement in the lateral and depth resolution of the technique [1]. This is very useful for the characterisation of materials which contain sub-micrometre phases, such as steel materials that have undergone heat treatment at high temperatures.

However, EPMA at low beam energies poses several difficulties which may affect the accuracy of quantitative results [1-3]. At low voltages, especially below 5 kV, the L-lines of the main metal components such as Fe, Ni and Cr have to be used because the higher energy K-lines cannot be excited but the reliability of EPMA using low energy L-lines is not yet as well advanced as when using the higher energy K-lines. Moreover, at low beam voltages, a surface layer of several nanometres in thickness represents a much larger fraction of the sample and, therefore, the influence of carbon contamination, surface oxidation, or the quality of the sample polish becomes more important [2, 3]. Unfortunately, there is a lack of systematic studies in which the performance of currently available EPMA systems are assessed at low voltage [4].

In this communication, we present the results of an inter-laboratory comparison of EPMA analysis at low voltage of three alloy steel samples. EPMA analyses of the samples were conducted by seven participant groups using electron microprobes and scanning electron microscopes (SEMs) of different manufacturers and models, equipped with wavelength- (WDS) and/or energy-dispersive X-ray systems (EDS), and their own methodology of analysis. The aim of the work was to obtain an estimate of the present situation of low-voltage analysis in the case of steels and identify needs for improvement.

2. Preparation and characterisation of alloy steel samples

2.1. Sample preparation and characterisation

AISI 316, AISI 310S and Incoloy 135 alloy samples were prepared from conventionally produced ingots of the corresponding alloys. The samples were treated so as to obtain a homogeneous structure and a condition equivalent to that of commercial products. Here it should be noted that none of the considered alloys are Ti or Nb stabilized. Thus, to avoid Cr carbide precipitation, the samples were subjected to a solubilisation heat treatment at a temperature of 1200 °C for 90 min, followed by water quenching. The samples finally were embedded in conductive resin and polished in a sequence of steps, finishing with 1 µm diamond on a hard cloth.

The bulk composition of the samples was determined using conventional techniques and procedures used in steel works. In particular, Si, Ti, Cr, Mn, Co, Ni, Cu, Nb, Mo and Sn were analyzed by X-ray fluorescence (XRF) using a Panalytical PW 2606 XRF spectrometer; B, Al, V and Pb were determined by optical emission spectroscopy (OES) using a Spectro 111982 spectrometer; and finally C and S, and N were analyzed by using Leco analysers CS 600 and TC 600. The Fe-content was obtained by difference to 100 %. The bulk composition of the three steel samples is given in table 1. Elements with conventional residual concentrations (< 0.05 wt%) such as B, N, C, Al, S, Ti, and Nb are not listed in the table.

Sample homogeneity was checked by performing 200 EDS analyses on each sample, which yielded standard deviation values (as $\pm 1\sigma$) less than 2 % for the major elements.

Preliminary EPMA-WDS analyses were performed on a Cameca SX-50 electron microprobe at an accelerating voltage of 20 kV, using $K\alpha$ -lines of Cr, Mn, Fe, Co, Ni and Cu, and they were found to be in satisfactory agreement with the reference values, with no systematic departures observed. The results of the preliminary analyses are summarized in table 2.

The samples were distributed to the participant laboratories, with no special guideline. The only instruction given was to perform the analyses at an accelerating voltage of 5 or 6 kV, with the procedures and conditions chosen by themselves.

Table 1. Composition of the three alloy samples (in wt%).

Sample	ID code	Si	Cr	Mn	Fe	Co	Ni	Cu	Mo
P11	AISI 316	0.483 (0.001)	17.18 (0.06)	1.483 (0.005)	66.51 (0.01)	0.336 (0.002)	11.24 (0.03)	0.309 (0.002)	2.163 (0.005)
P13	AISI310S	1.340 (0.008)	25.0 (0.1)	1.610 (0.006)	50.61 (0.01)	0.050 (0.001)	20.02 (0.04)	0.750 (0.004)	0.400 (0.001)
P15	Incoloy 135	0.58 (0.02)	28.3 (0.2)	0.74 (0.02)	25.7 (0.2)	0.030 (0.002)	39.7 (0.3)	1.54 (0.03)	3.10 (0.04)

Numbers in parentheses are one standard deviation uncertainties.

Table 2. Results of preliminary WDS analysis at 20 keV.

Sample	Si	Cr	Mn	Fe	Co	Ni	Cu	Mo	Total
P11	0.53 (0.01)	17.8 (0.3)	1.47 (0.03)	66.0 (0.6)	0.32 (0.01)	11.03 (0.4)	0.30 (0.02)	2.27 (0.06)	99.76
P13	1.42 (0.04)	25.33 (0.3)	1.58 (0.05)	50.6 (0.7)	0.03 (0.01)	19.5 (0.3)	0.75 (0.03)	0.4 (0.03)	99.67
P15	0.60 (0.08)	29.4 (0.4)	0.71 (0.09)	24.6 (0.7)	0.0	39.4 (0.7)	1.6 (0.1)	3.3 (0.3)	99.69

3. Experimental conditions of analysis

3.1. Wavelength-dispersive X-ray spectrometry

The equipment and experimental conditions used by the participants are summarized in table 3. All analyses were performed at an accelerating voltage of 6 kV, with the exception of laboratory 6 which used 5 kV. Most of the measurements were performed on electron microprobes (Cameca SX-50, SX-51 and SX-100); only one measurement was performed on a SEM equipped with WDS (Leo 1450). Different dispersing crystals were used, which include TAP, LTAP, PET, LPET, PC0, and PC1, with different pulse-height analyzer settings (in integral and differential mode). All participants used pure reference standards for calibration purposes. The correction procedures used were PAP, XPP and XPHI. Three participants polished the standards and samples before analysis (to remove a possible oxide and contamination layer) and one participant coated samples and standards with a carbon layer. A liquid N₂ trap was used by three laboratories to minimize carbon contamination during the measurements.

All participants obtained the net peak intensity by means of the standard procedure, e.g., by measuring the counting rate at the channel that corresponds to the peak maximum and subtracting the spectral background by linear interpolation of two measurements performed at both sides of the peak. For Cr, multiple background measurements with curved background modelling were performed by participant 6 and participant 1 used parabolic interpolation instead of linear interpolation. Each laboratory performed 10 measurements on each sample, except laboratory 4, which performed 20 measurements.

Table 3. Equipment and experimental conditions used in the WDS analyses.

Lab code	Instrument	Current (nA)	Crystals and Elements	Standards	Correction procedure	Specimen treatment	Remarks
1	Cameca SX-50	100	TAP: Cu, Ni, Fe, Mn, Si PET: Mo PC1: Cr	Pure*	PAP	Polishing	L-N ₂ trap
2	Cameca SX-100	200	TAP: Cu, Ni, Fe, Mn, Si LPET: Mo PC1: Cr	Pure*	XPHI	Polishing	L-N ₂ trap
3	Leo 1450 Inca Wave	40	PET: Si, Mo TAP: Cu, Ni, Fe, Mn, Cr	Pure	XPP	None	
4	Cameca SX-50	50	PC1: Cr, Fe TAP: Mn, Ni, Co, Cu PET: Si, Mo	Pure*	PAP	Polishing	
5	Cameca SX-100	200	LTAP: Si, Cr, Mn, Fe, Ni, Cu LPET: Mo	Pure	XPHI	None	
6	Cameca SX-51	40	TAP: Si PC1: Cr PC0: Mn, Fe, Ni, Co PET: Mo	Pure	PAP	Carbon coating. No polishing	L-N ₂ trap. Multiple backgrounds

* Standards were polished before analysis.

3.2. Energy-dispersive X-ray spectrometry

The equipment and the experimental conditions are summarized in table 4. All analyses were performed at an accelerating voltage of 6 kV, with the exception of laboratory 1 which used 5 kV. Laboratory 1 used two different instruments, which are referred in the table to as 1a and 1b. Participant 4 used simultaneously two SDDs mounted on the same SEM to improve statistics. EDS analyses were performed with and without standards, and were reported as non-normalized and normalized. Only non-normalized results have been considered here. Each laboratory performed 10 measurements on each sample, except laboratory 1, which performed 100 measurements.

4. Results

4.1. Wavelength-dispersive X-ray spectrometry

Representative X-ray spectra recorded at 6 kV around the positions of the Cr L α -, Fe L α - and Ni L α -lines emitted from pure Cr, Fe and Ni reference samples, as well as from samples P11 (Cr, Ni) and P15 (Fe) are shown in figure 1. The spectra from the steel samples have been normalized to the peak maxima from the corresponding pure metal samples to facilitate comparison. The dispersing crystals used are PC1 (for Cr) and TAP (for Fe and Ni).

In the case of Fe and Ni, differences are observed in the high-energy tails of the L α and L β peaks when comparing the spectra recorded from the pure standards with those recorded from the steel samples. These differences are most likely due to different self-absorption, as the latter effect depends on sample composition (the L₃ absorption edges are located at 574 eV for Cr, 707 eV for Fe and 854 eV for Ni). Due to the lower spectral resolution of the PC1 crystal, the L α - and L β -lines of Cr could not be resolved.

Table 4. Equipment and experimental conditions used in the EDS analyses.

Lab Code	Instrument	Current (nA)	EDS	Standards	Correction procedure	Sample treatment	Other remarks
1a	FEG-SEM Leo 982	2.7	SDD INCA	Standardless	XPP	Plasma cleaning	Beam voltage: 5 kV
1b	FEG-SEM Zeiss Ultra 55	1.8	Si(Li) INCA	Standardless	XPP	Plasma cleaning	Beam voltage: 5 kV
2	Cameca SX-50	2	SDD SAMx	Pure*	XPP	Polishing	
3	SEM Leo 1450		SDD INCA	Pure	XPP	None	
4	SEM Jeol 7001F	1.46	2 SDDs Thermo Scientific	Pure	PROZA	None	2 SDDs used simultaneously

*Standards were polished before analysis.

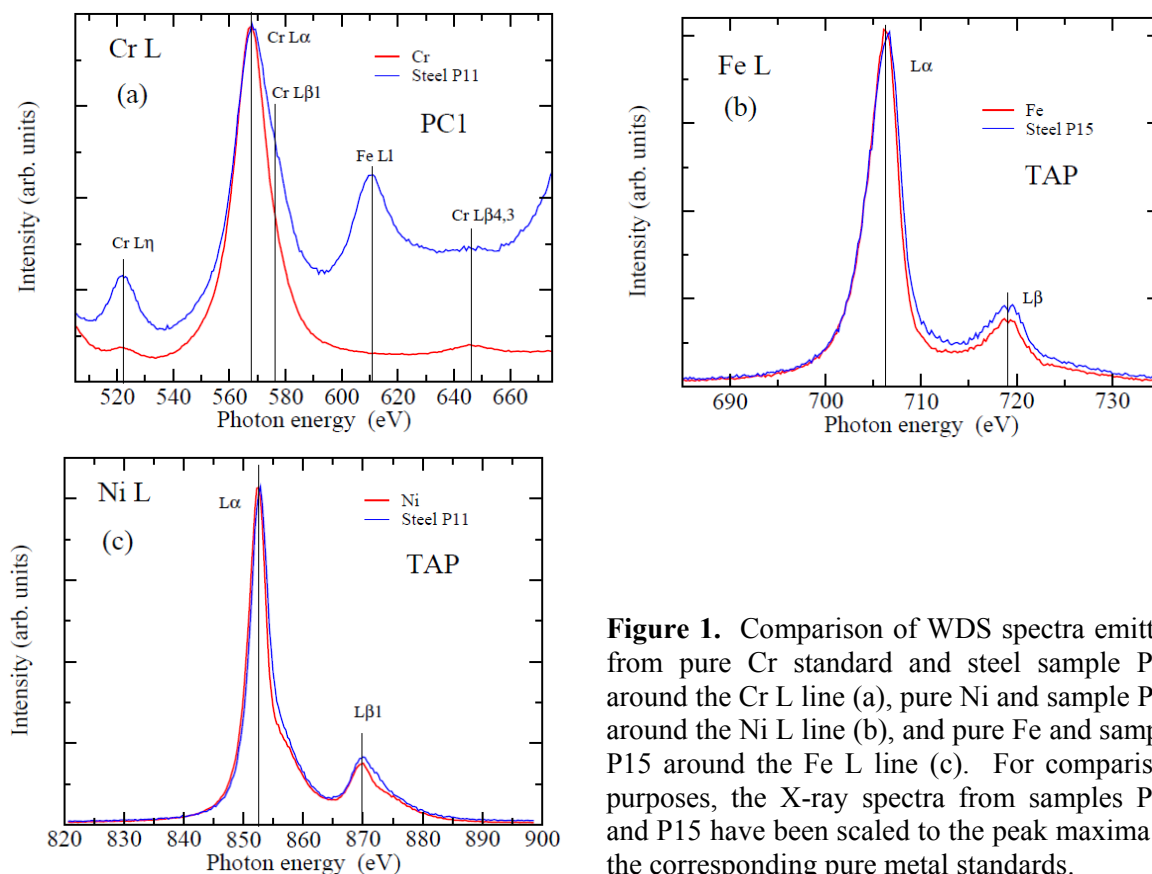


Figure 1. Comparison of WDS spectra emitted from pure Cr standard and steel sample P11 around the Cr L line (a), pure Ni and sample P11 around the Ni L line (b), and pure Fe and sample P15 around the Fe L line (c). For comparison purposes, the X-ray spectra from samples P11 and P15 have been scaled to the peak maxima of the corresponding pure metal standards.

The results of the WDS analyses of the P11, P13 and P15 samples are summarized in tables 5, 6 and 7, along with the standard deviations reported by the participants. The latter were calculated from the number of measurements performed, which is indicated above. The negative Co concentrations reported, which obviously have no physical meaning, are an indication of measurement difficulties

(e.g., in background subtraction) found for this element. The sum of the measured concentrations ranged from 100.2 and 124.6 wt%.

Table 5. Results of quantitative WDS analyses of the P11 sample (all values in wt%).

Lab code	Si	Cr	Mn	Fe	Co	Ni	Cu	Mo	Total
Reference composition	0.483	17.18	1.483	66.51	0.336	11.24	0.309	2.163	
1	0.57 (0.02)	14.42 (0.27)	0.88 (0.25)	66.65 (0.7)	0.38 (0.04)	14.65 (0.43)	0.35 (0.03)	2.39 (0.10)	100.29
2	0.52 (0.01)	15.77 (0.14)	1.10 (0.11)	67.86 (0.5)	0.4 (0.05)	14.45 (0.27)	0.35 (0.02)	2.16 (0.04)	102.59
3	0.39 (0.02)	14.33 (0.82)	0.21 (0.28)	86.25 (1.24)	0.27 (0.05)	15.33 (0.53)	0.34 (0.01)	7.54 (0.24)	124.64
4	0.46 (0.06)	15.24 (0.35)	1.49 (0.54)	70.04 (0.3)	0.31 (0.16)	16.0 (0.6)	0.35 (0.06)	2.25 (0.15)	106.14
5	0.50 (0.004)	14.82 (0.77)	1.03 (0.06)	72.97 (0.5)	-0.04 (0.04)	15.13 (1.6)	0.39 (0.06)	2.15 (0.05)	106.99
6	0.51 (0.05)	16.91 (0.64)	0.24 (0.63)	70.36 (0.81)	“Not measured”	14.04 (0.36)	0.59 (0.18)	2.16 (0.35)	104.80

Numbers in parentheses are one standard deviation uncertainties.

Table 6. Results of quantitative WDS analyses of the P13 sample (all values are in wt%).

Lab	Si	Cr	Mn	Fe	Co	Ni	Cu	Mo	Total
Reference composition	1.340	25.0	1.610	50.61	0.050	20.02	0.750	0.400	
1	1.52 (0.05)	21.34 (0.16)	1.03 (0.16)	50.87 (0.73)	0.00	24.97 (0.16)	0.93 (0.04)	0.48 (0.05)	101.15
2	1.38 (0.08)	22.59 (0.35)	1.16 (0.09)	50.8 (1.02)	-0.04 (0.03)	25.11 (0.32)	0.86 (0.04)	0.4 (0.04)	102.3
3	1.15 (0.06)	21.05 (0.60)	0.52 (0.22)	65.02 (1.88)	0.00	25.87 (1.70)	0.79 (0.08)	1.45 (0.18)	115.84
4	1.34 (0.10)	22.99 (0.52)	1.72 (0.63)	56.37 (0.80)	0.06 (0.08)	25.84 (0.65)	0.8 (0.11)	0.47 (0.15)	109.58
5	1.44 (0.06)	20.71 (2.71)	1.26 (0.05)	55.98 (1.04)	-0.14 (0.06)	26.09 (0.35)	0.99 (0.05)	0.43 (0.03)	106.9
6	1.38 (0.1)	23.83 (1.00)	0.0	56.29 (0.81)	“Not measured”	24.57 (0.4)	1.1 (0.13)	0.37 (0.27)	107.5

Numbers in parentheses are one standard deviation uncertainties.

The results of the six participants are in good agreement with each other within a relative standard deviation of 10 % (Si), 7 % (Cr), 9 % (Fe), 3 % (Ni), and 16 % (Cu). For Mn and Mo the agreement is within 60 % and 70 %, respectively. For the latter element, the results from participant 3 are a factor of 4 larger than the other participants and, therefore, a problem with this element is suspected. The results for Co are meaningful only for sample P11; in this case, the results from all participants agree with each other to within 68 %.

Table 7. Results of quantitative WDS analyses of the P15 sample (all values are in wt%).

Lab code	Si	Cr	Mn	Fe	Co	Ni	Cu	Mo	Total
Reference composition	0.58	28.3	0.74	25.7	0.030	39.7	1.54	3.10	
1	0.59 (0.07)	23.91 (0.49)	0.47 (0.17)	24.65 (0.76)	0.00	47.12 (0.48)	1.74 (0.12)	3.37 (0.35)	102.44
2	0.49 (0.05)	26.07 (0.39)	0.49 (0.14)	26.06 (0.41)	-0.25 (0.05)	47.77 (0.26)	1.66 (0.10)	2.76 (0.21)	105.29
3	0.65 (0.03)	24.46 (1.27)	0.00	29.44 (0.63)	0.00	47.02 (1.23)	1.72 (0.05)	13.01 (0.47)	116.30
4	0.57 (0.13)	27.03	0.46 (0.53)	28.62 (1.17)	0.03 (0.06)	46.48 (0.58)	1.69 (0.20)	3.38 (0.57)	108.25
5	0.59 (0.13)	23.37	0.51 (0.12)	26.89 (1.32)	0.15 (0.05)	48.41 (0.80)	2.02 (0.22)	3.26 (1.57)	105.20
6	0.62 (0.10)	28.12 (2.10)	0.00	27.44 (4.9)	Not measured	45.48 (2.28)	2.06 (0.41)	3.71 (1.28)	106.60

Numbers in parentheses are one standard deviation uncertainties.

Figure 2 shows comparison results in a graphical form for Cr, Fe and Ni, as function of participant code for sample P13. The error bars correspond to the claimed one standard deviation uncertainties. For comparison purposes, the reference values, as well as the average and error bands (at 2σ level) are also displayed. The scattering of results is large as compared to what is usual in EPMA round robins.

The relative variation ΔC of each measurement C_{meas} with respect the reference value C_{ref} was calculated as

$$\Delta C = (C_{\text{meas}} - C_{\text{ref}}) / C_{\text{ref}} \times 100, \quad (1)$$

and the results for Cr, Fe and Ni are shown in table 8. The results show a systematic underestimation of the Cr contents, with relative deviations from the reference values ranging from -0.8 % to -17.5 %, and an overestimation of Fe and Ni, with relative deviations ranging from -4.2 % to +29.6 %, and from +14.4 % to +42.4 %, respectively.

Table 8. Relative deviations (in %) from the reference concentrations for Cr, Ni, Fe for each laboratory. See text for details.

Lab. no.	P11			P13			P15		
	Cr	Fe	Ni	Cr	Fe	Ni	Cr	Fe	Ni
1	-16.1	0.2	30.3	-14.5	0.5	24.7	-15.6	-4.2	18.5
2	-8.2	2.0	28.5	-9.6	0.4	25.4	-8.0	1.3	20.2
3	-16.6	29.7	36.4	-15.7	28.5	29.2	-13.7	14.5	18.3
4	-11.32	5.3	42.4	-8.1	11.4	29.1	-4.6	11.2	17.0
5	-13.8	9.7	34.6	-17.1	10.6	30.3	-17.5	4.5	22.0
6	-1.6	5.8	25.0	-4.6	11.2	22.7	-0.8	6.7	14.4

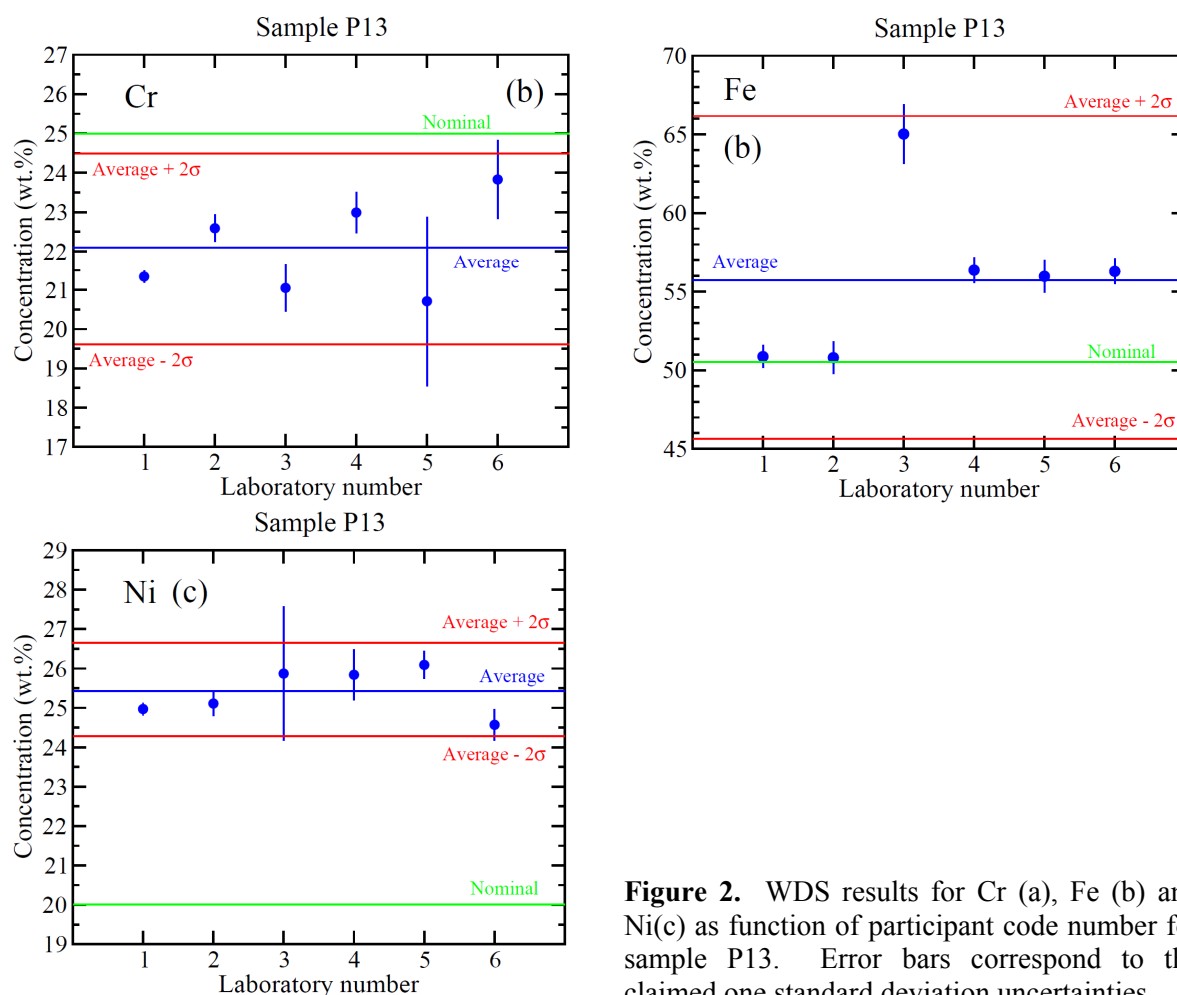


Figure 2. WDS results for Cr (a), Fe (b) and Ni(c) as function of participant code number for sample P13. Error bars correspond to the claimed one standard deviation uncertainties.

4.2. Energy-dispersive X-ray spectrometry

EDS spectra recorded at an accelerating voltage of 6 kV on samples P11 and P15 are shown in figure 3. The spectra show severe peak overlaps for most of the metal L-lines below a photon energy of 1 keV.

The results of the EDS analyses of the P11, P13 and P15 samples are summarized in tables 9, 10 and 11, together with the standard deviations reported by the participants. Although normalized and non-normalized results were reported, only non-normalized values are shown in the tables. In some cases, it was not possible to detect Co and Mn due to the heavy overlap of the major elements. The relative deviations obtained by using EDS, calculated by using Eq. 1, showed larger scatter than for WDS, ranging from -16 % to +54 % for Cr, -0.4 % to +66 % for Fe and from +13 % to +90 % for Ni.

5. Discussion

In the case of the measurements performed by WDS, the participant laboratories used quite different experimental parameters and matrix correction procedures (see table 3). However, similar systematic deviations for the Cr, Ni and Fe concentrations are observed, except in the case of Fe measured by laboratory 3, for which much larger deviations are observed (see table 8). The reasons for such larger deviations are attributed to a deficient Fe standard. The fact that three participants polished samples and standards before analysis and used an anti-contamination device (liquid N₂) suggests that the reason for the systematic deviation might not be due (at least only) to the presence of an oxide layer

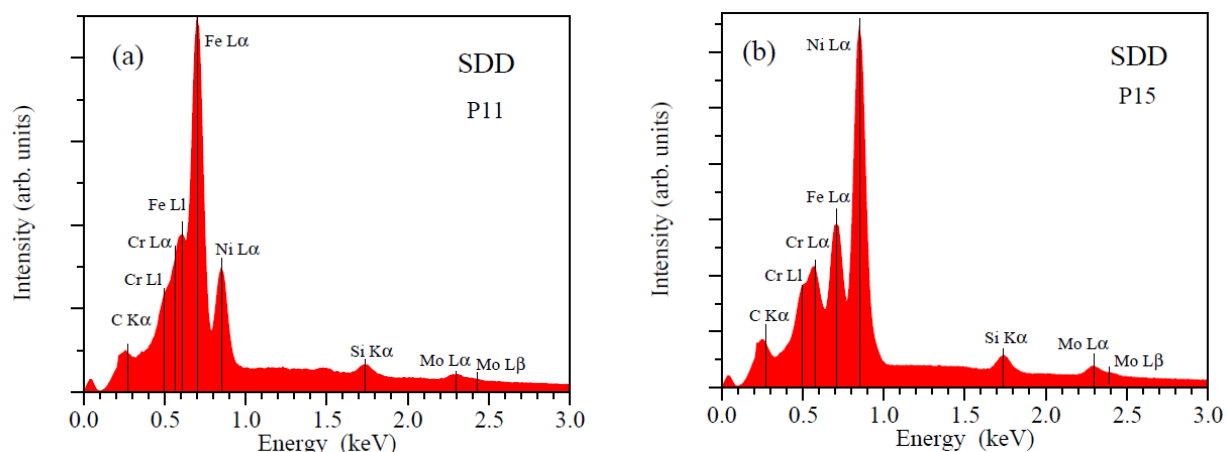


Figure 3. EDS spectra obtained with a SDD detector from samples P11 (a) and P15 (b) at 6 kV.

Table 9. Results of quantitative EDS analyses of the P11 sample (all values are in wt%). Numbers in parentheses are one standard deviation uncertainties.

Lab code	Si	Cr	Mn	Fe	Co	Ni	Cu	Mo	Total
Reference composition	0.483	17.18	1.483	66.51	0.336	11.24	0.309	2.163	
1a	0.67 (0.08)	36.00 (1.39)	-6.21 (1.16)	104.22 (9.04)	-1.87 (0.68)	21.42 (2.47)	0.18 (0.46)	2.82 (0.40)	157.25
1b	0.53 (0.07)	28.98 (0.86)	-1.05 (1.30)	100.10 (1.24)	1.02 (0.55)	18.53 (0.62)	0.09 (0.21)	2.83 (0.38)	151.04
2	0.44 (0.09)	26.13 (0.45)	0.00	76.98 (0.38)	0.00	13.90 (0.42)	0.39 (0.15)	1.68 (0.11)	119.52
3	0.60 (0.04)	23.26 (0.69)	0.47 (1.00)	85.22 (1.07)	2.78 (0.48)	17.26 (0.35)	0.03 (0.10)	5.39 (0.27)	135.00
4	0.70 (0.04)	10.25 (0.31)	0.0	73.75 (0.65)	0.0	16.93 (0.19)	0.31 (0.10)	2.54 (0.27)	104.47

Numbers in parentheses are one standard deviation uncertainties.

(native oxide layer on the standards and/or passive layer on the steel samples) or to carbon contamination effects. Likewise, it seems plausible not to attribute the observed discrepancies to only background subtraction errors, since very different background “positions” and methods were used by the participants. However, it should be noted that all the participants measured peak intensities and not peak areas in order to extract the X-ray intensities. As a result, possible systematic errors due to peak shape changes between standards and the analyzed steel samples cannot be ruled out. The use of standards with similar composition as those of the analyzed specimens would shift the observed deviations to smaller values, as possible shortcomings of matrix correction procedures and/or measurement errors would be minimized.

In the case of EDS analysis, the results obtained are most likely affected by large systematic errors in the extraction of X-ray intensities due to severe peak overlapping. As a result, only the results obtained by WDS will be considered in the following discussion.

Table 10. Results of quantitative EDS analyses of the P13 sample (all values are in wt%). Numbers in parentheses are one standard deviation uncertainties.

Lab code	Si	Cr	Mn	Fe	Co	Ni	Cu	Mo	Total
Reference composition	1.340	25.0	1.610	50.61	0.050	20.02	0.750	0.400	
1a	1.57 (0.11)	43.92 (1.23)	-7.40 (0.80)	82.19 (1.51)	-3.77 (0.47)	37.96 (0.65)	1.05 (0.20)	0.66 (0.29)	156.17
1b	1.44 (0.12)	38.26 (0.97)	-1.39 (1.00)	80.21 (1.63)	0.38 (0.58)	32.66 (0.68)	0.67 (0.24)	0.62 (0.32)	152.86
2	1.32 (0.07)	31.54 (0.61)	0.00	63.39 (0.76)	0.00	24.85 (0.15)	0.66 (0.09)	0.25 (0.08)	122.02
3	1.48 (0.04)	30.39 (0.35)	1.08 (1.41)	67.77 (0.71)	2.39 (0.41)	28.87 (0.27)	0.59 (0.12)	0.93 (0.39)	133.51
4	1.61 (0.06)	18.43 (1.19)	0.01	58.90 (0.50)	0.00	28.91 (0.47)	1.12 (0.09)	0.54 (0.25)	109.50

Numbers in parentheses are one standard deviation uncertainties.

Table 11. Results of quantitative EDS analyses of the P15 sample (all values are in wt%). Numbers in parentheses are one standard deviation uncertainties.

Lab code	Si	Cr	Mn	Fe	Co	Ni	Cu	Mo	Total
Reference composition	0.58	28.3	0.74	25.7	0.030	39.7	1.54	3.10	
1a	0.66 (0.12)	43.74 (1.63)	-6.10 (0.76)	41.15 (2.05)	-5.14 (0.47)	70.62 (1.75)	2.38 (0.37)	4.07 (1.05)	151.38
1b	0.58 (0.13)	41.51 (1.44)	-1.31 (0.73)	42.84 (2.11)	1.08 (0.58)	62.73 (1.55)	1.56 (0.35)	4.10 (0.82)	153.09
2	0.52 (0.04)	30.73 (0.21)	0.00	30.97 (1.16)	0.91 (0.01)	49.23 (0.41)	0.83 (0.12)	2.67 (0.19)	114.95
3	0.64 (0.12)	35.05 (0.97)	1.15 (0.23)	37.81 (1.42)	2.74 (0.35)	54.82 (0.65)	1.47 (0.30)	7.70 (1.36)	141.41
4	0.76 (0.07)	23.64 (1.28)	0.00	29.92 (0.91)	0.00	52.82 (0.52)	2.33 (0.09)	3.45 (0.08)	112.93

Numbers in parentheses are one standard deviation uncertainties.

5.1. Matrix correction procedures

In order to assess the effect of using matrix correction procedures different from those used by the participants, one set of results (laboratory 1, sample P13) was recalculated using different $\phi(\rho z)$ -based procedures, namely the PROZA model, and those of Packwood and Armstrong, with the help of the code CALCZAF (details on the tested correction procedures as implemented in CALCZAF can be found in Ref. [5]). For all the tested correction procedures, the same set of MACs was used, namely the FFAST compilation [10]. As shown in table 12, the use of different correction procedures resulted in only small changes of the Cr, Ni and Fe concentrations. Here it should be pointed out that fluorescence effects are almost negligible for the L-lines of the considered elements, owing to their extremely low fluorescence yields.

Table 12. Comparison of WDS results (in wt%) for different correction procedures using the FFAST MACs (k -ratios measured on sample P13 by laboratory 1).

Correction procedure/MAC	Si	Cr	Mn	Fe	Ni	Cu	Mo	Total
Reference composition	1.340	25.0	1.610	50.61	20.02	0.750	0.400	
PROZA/FFAST	1.47	22.4	1.07	51.6	25.2	0.87	0.44	103.13
Packwood/FFAST	1.46	22.5	1.09	52.7	26.6	0.93	0.45	105.80
Armstrong/FFAST	1.54	22.7	1.10	52.6	26.0	0.89	0.43	105.28

5.2. Mass absorption coefficients

Although the use of different correction procedures yields small changes in the evaluated concentrations, a problem with a matrix correction parameter such as the mass-attenuation coefficient (MAC) cannot be excluded.

Different MACs are available for the Cr, Fe and Ni $L\alpha$ X-ray lines in Cr, Fe and Ni respectively, which are summarized in table 13. This table also includes values obtained empirically by Pouchou and Pichoir [12] and by participant 1, using the programme XMAC [3], from measurements on pure Cr, Fe and Ni samples up to 20 kV. For a given X-ray line and element, the mentioned programme determines the MAC by i) considering it as a free parameter in the XPP model, and ii) fitting the predictions of the model to measurements of the X-ray intensity as a function of beam energy. In the case of Cr, the $L\alpha$ and $L\beta$ peaks appear as a single ($L\alpha+L\beta$) line, therefore, the use of the L doublet for analysis will lead to an additional source of uncertainty, as the MAC for the $L\alpha$ line differs significantly from that of the $L\beta$ line (see e.g., Ref [11]).

Table 13. MACs for Cr, Fe and Ni $L\alpha$ X-rays in Cr, Fe and Ni, respectively, taken from different compilations (in cm^2/g).

Source	Cr $L\alpha$	Fe $L\alpha$	Ni $L\alpha$
LINEMU: Henke [6], Heinrich [7]	2611	2146	1819
CITZMU: Heinrich [7], Henke and Ebisu [8]	2612	2149	1801
MAC30: Heinrich [9]	2650	2157	1806
FFAST: Chantler et al. [10]	2395	1967	1697
Empirical: Pouchou and Pichoir [12]	3850	3350	3560
Empirical: This work	3612	3559	4277

To assess the effect of using different MACs on the resulting concentrations, the k -ratios obtained by laboratory 1 for sample P13 were re-evaluated using the PAP model with the MACs shown in table 13. The results are summarized in table 14 and indicate that the use of empirical MACs gives results closer to the reference values for Fe and Ni, although for the latter element they are still far off. Transition metals such as Fe, Cr and Ni are known to have a narrow and partially empty 3d band and, as a result, the MAC in the vicinity of the L_3 edge changes rapidly with photon energy [13]. These large fluctuations are not accounted for in most available compilations. The use of empirical MACs obtained from EPMA measurements provides a convenient way to overcome, at least partially, this difficulty.

Table 14. Comparison of WDS results (in wt%) for the PAP correction procedure using different MACs (results from sample P13, laboratory 1).

Correction procedure/MAC	Si	Cr	Mn	Fe	Ni	Cu	Mo	Total
Reference composition	1.340	25.0	1.610	50.61	20.02	0.750	0.400	
PAP/LINEMU	1.51	22.7	1.09	52.8	26.3	0.92	0.44	105.91
PAP/CITZMU	1.53	22.8	1.10	52.9	26.5	0.91	0.44	106.27
PAP/MAC30	1.52	22.6	1.09	53.0	26.9	0.94	0.45	106.62
PAP/FFAST	1.50	22.6	1.10	52.7	26.4	0.91	0.44	105.74
PAP/Pouchou	1.51	21.3	1.02	50.6	24.3	0.91	0.44	100.22
PAP/This work	1.51	21.6	1.03	50.5	23.5	0.91	0.45	99.49

5.3. Measurement of *k*-ratios at different beam energies

To further elucidate the source of the observed discrepancies, *k*-ratio measurements at varying voltages in the range 4 - 20 kV were performed on samples P11, P13 and P15 by laboratory 1. The experimental *k*-ratios are compared in figure 4 with the predictions of the PAP model, using MACs from Ref. [12] (continuous line). For Fe, the agreement between the experimental measurements with the PAP model seems to be satisfactory. Figure 4 also displays the predictions of the PAP model for Ni and Cr re-scaled such that they match the experimental measurements at 4 keV (dashed lines). For the mentioned elements, the differences between the experimental data and the re-normalized PAP results seem to slightly increase with increasing beam energy, which could indicate an absorption anomaly. Although the metals considered here should be in the same chemical state as pure elements (since steel is a solid solution, i.e., with no inter-metallic phases or oxides), we cannot rule out the possibility that the proximity of neighbouring atoms could modify the MACs of the L-lines of these metals. Here it should be pointed out that the modulation of the absorption coefficient by neighbouring atoms is the basis of the well established EXAFS technique.

5.4. Measurements of other alloy steel samples

Further measurements were performed at 6 kV by laboratory 1 on other steel samples of known composition, with Cr, Fe and Ni contents ranging from 1.16 - 28.3 wt%, 25.7 - 96.4 wt% and 0.10 - 39.7 wt%, respectively (see table 15 for reference compositions). For the sake of completeness, table 15 also includes the composition of the P11, P13 and P15 materials.

The results of these measurements for Cr and Ni are displayed in figure 5. As it can be seen, the differences observed between the measured and the reference concentrations increase with increasing concentration, thus confirming the tendencies observed for samples P11, P13 and P15.

Table 15. Concentration of Cr, Fe and Ni (in wt%) of 15 alloy steel reference samples.

	P01	P02	P03	P04	P05	P06	P07	P08	P09	P10	P11	P12	P13	P14	P15
Cr	1.16	4.94	11.4	16.1	17.0	17.3	18.3	18.1	17.4	13.7	17.2	12.4	25.0	23.5	28.3
Fe	96.4	93.6	86.1	65.7	67.3	69.7	70.6	67.6	70.8	72.1	66.5	70.7	50.6	51.5	25.7
Ni	0.10	0.11	0.80	1.52	2.61	4.51	8.13	8.61	9.30	9.92	11.2	14.8	20.0	21.7	39.7

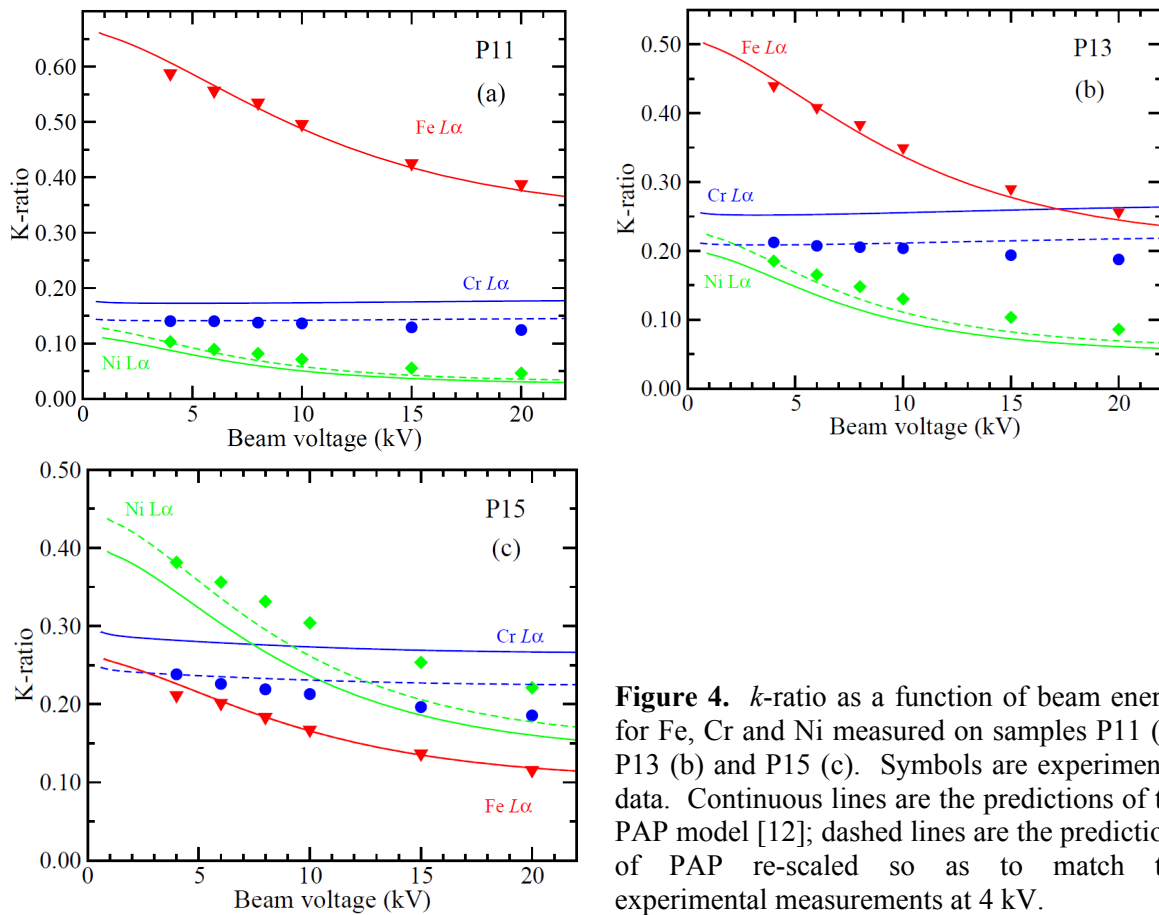


Figure 4. k -ratio as a function of beam energy for Fe, Cr and Ni measured on samples P11 (a), P13 (b) and P15 (c). Symbols are experimental data. Continuous lines are the predictions of the PAP model [12]; dashed lines are the predictions of PAP re-scaled so as to match the experimental measurements at 4 kV.

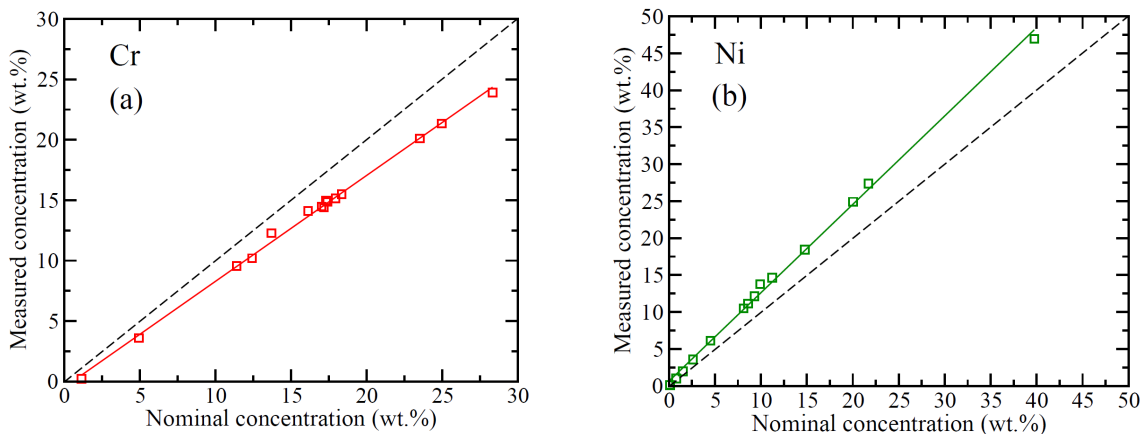


Figure 5. Measured versus reference concentration for Cr (a) and Ni (b) obtained in a series of 15 alloy steel samples with varying Cr and Ni concentrations (see table 15). Symbols are experimental measurements. Continuous lines represent the results of linear regression. Beam voltage is 6 kV.

6. Conclusion

Despite the participant laboratories having used quite different experimental conditions and matrix correction procedures for the WDS analysis, similar systematic deviations in the Cr, Fe and Ni concentrations have been observed. Inaccuracy of the adopted MACs for the L-lines of the metal elements as well as experimental errors in the extraction of X-ray intensities are believed to be the main sources of uncertainty. In the case of EDS analysis, the results obtained are most likely affected by large systematic errors due to severe peak overlapping. Further work is needed for accurate quantitative EPMA analysis of alloy steel at low beam voltage.

References

- [1] Newbury D E 2002 *J. Res. Natl. Inst. Stand. Technol.* **107** 605
- [2] Willich P and Bethke R 1996 *Mikrochim. Acta Suppl.* **13** 631
- [3] Pouchou J L 1996 *Mikrochim. Acta Suppl.* **13** 39
- [4] Briant M and Balloy D 2008 *Eur. Phys. J. Appl. Phys.* **44** 37
- [5] Probe Software Inc., available on-line: <http://www.probesoftware.com/Technical.htm>
- [6] Henke B L, Lee T J, Tanaka R J, Shimabukuro R L and Fijikawa B K 1985 *Atomic Data Nucl. Data Tables* **27** 1
- [7] Heinrich K F J 1966 *The electron microprobe*. McKinley T D, Heinrich K F J and Wittry D B, eds. (New York: John Wiley and Sons) pp. 1035
- [8] Henke B L and Ebisu E S 1974 *Adv. X-ray Anal.* **17** 150
- [9] Heinrich K F J 1986 *Proc. 11th International Congress on X-ray Optics and Microanalysis*. Brown J D and Packwood R H, eds. (Ontario: University of Western Ontario)
- [10] Chantler C T, Olsen K, Dragoset R A, Chang J, Kishore A R, Kotochigova S A and Zucker D S 2005 *X-ray form factors, attenuation and scattering tables (version 2.1)*. Available online: <http://physics.nist.gov/ffast>
- [11] Rickerby D G and Wachter N 2000 *Mikrochim. Acta* **132** 157
- [12] Pouchou J L and Pichoir F 1991 *Electron probe quantitation*. Heinrich K F J and Newbury D E. (New York: Plenum Press), pp. 31
- [13] Chopra D 1970 *Phys. Rev. A* **1** 230